CRATER RELAXATION AND STEREO IMAGING OF RHEA. N. P. Hammond[1], C. B. Phillips[1] , G. Robuchon[2], R. Beyer[1,3] , F. Nimmo[2] and J. Roberts[4]. [1]SETI Institute, Mountain View, CA; nhammond@seti.org, [2]University of California at Santa Cruz [3]NASA Ames Research Center [4]John Hopkins University Applied Physics Laboratory

Summary: Over billions of years, craters reduce in depth at a rate that is dependent on internal properties of the target body. Thus measuring the depth of craters can give insight into the thermal history and subsurface structure of terrestrial bodies and icy satellites. [1]. Extensive surface coverage provided by Cassini and automated stereo-imaging programs now allow for more reliable measurements of crater depths on the moons of Saturn, and thus more accurate estimates of crater relaxation. We utilize these resources to create digital elevation models of large craters (D>70km) on Rhea. Our topographic measurements serve as input into a coupled thermal evolution-viscoelastic relaxation code, allowing us to investigate the thermal history of Rhea. So far, our numerical simulations under-predict the amount of crater relaxation we observe, suggesting Rhea is warmer than we initially modeled.

Stereo Imaging: Overlapping image pairs of Rhea from the Cassini dataset were downloaded from the NASA Planetary Data System. ISIS software was used to determine the spacecraft's position relative to the surface and to attach geographic information to the image [2]. A network of control points was selected to calibrate the images to the same viewing geometry and to correct camera pointing information.

Once the images were tied together and reprojected to the same resolution, we used the Ames Stereo Pipeline [3] (ASP), to create digital elevation models (Figure 1). ASP is an automated stereo tool which identifies corresponding pixels and uses triangulation to calculate their vertical positions.

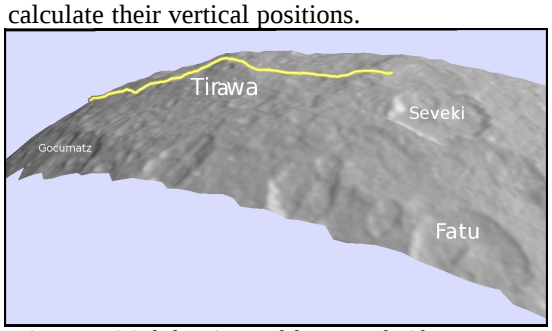

Figure 1: Digital elevation model generated with Ames Stereo Pipeline. Crater profile of Tirawa is indicated by yellow line.

Using an automated stereo program to measure crater depth has some advantages over alternative techniques, such as photoclinometry and measuring shadow lengths. The former requires no intrinsic albedo variation across the surface and the latter assumes the crater floor is flat [4]. Stereo requires neither of these assumptions and should give the most accurate estimate of topography.

Eight image pairs were used to extract 18 crater profiles. To test the validity of our methods, we measured two craters twice using separate stereo pairs and found very similar depths (within 10%).

Crater Relaxation: Crater relaxation is defined as the change in depth since formation divided by initial depth. Estimating the initial depth of complex craters is problematic and can only done by making certain assumptions. [4] measured the depths of small, fresh-looking craters on Rhea to extrapolate the initial depth of larger craters. This assumes that small craters behave the same as large complex craters which is probably not the case [5]. We employed a method used by [6] and calculated initial crater depths by assuming that Herschel crater on Mimas is completely unrelaxed and using scaling laws to adjust for changes in gravity and crater diameter [7, 8].

With this technique, we found that craters larger than 250 km in diameter, including Tirawa, are approximately 40% relaxed (Figure 2), suggesting that they could have formed very early in Rhea's history. Other craters less than 150 km in diameter range from 0 to 45% relaxed, suggesting a large variation of crater ages that is consistent with impact flux models [9].

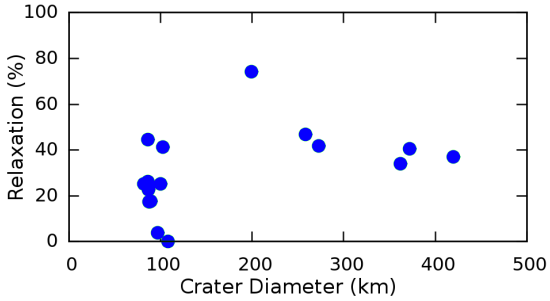

Figure 2: Observed crater relaxation versus crater diameter.

Thermal-Viscoelastic Model: Rhea is modeled as a 3-D spherical shell with equations for conservation of mass, momentum and energy applied. We assume Rhea is undifferentiated with a silicate density of 3510 kg m^3, an ice density of 920 kg m^3 and an 11% rock volumetric fraction of silicates [10]. The surface temperature is set to 90 K and is kept constant during the simulation. The initial temperature profile is computed by assuming that 40% of the accretion energy is retained as heat [11]. We use an accretion time of 2.9 Myr and a concentration of 37.5 ppb for 26Al, based on typical elemental abundances in ordinary chondrites [12, 13].

The model shows that the internal temperature peaks around 270 K at 10 Myr due to the decay of radioactive isotopes. Convection, a proxy for relax-

ation, is most vigorous from 0 to 1 Gyr and becomes negligible after 2 Gyr (Figure 3).

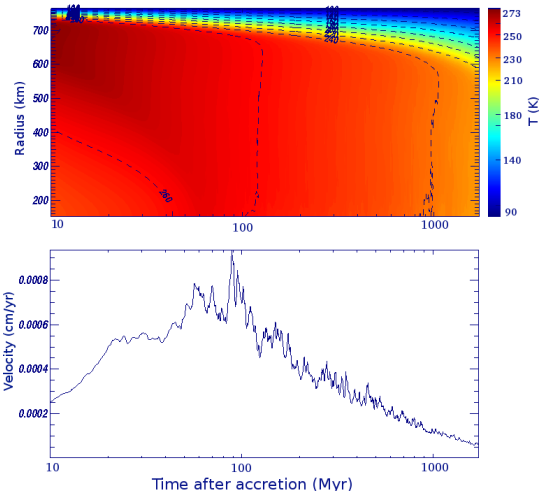

Figure 3a: Temperature with depth over time. 3b: Convective velocity over time.

A time-dependent viscosity structure, calculated by our thermal evolution model, serves as input into an axial-symmetric viscoelastic relaxation model [14]. Using this approach, we investigated the expected degree of relaxation for a 100 km diameter (Figure 4, green curve) and a 400 km diameter (Figure 4, red curve) crater formed at various ages. Our model predicts a maximum of 10% and 40% relaxation for a 100 km and 400 km diameter crater, respectively.

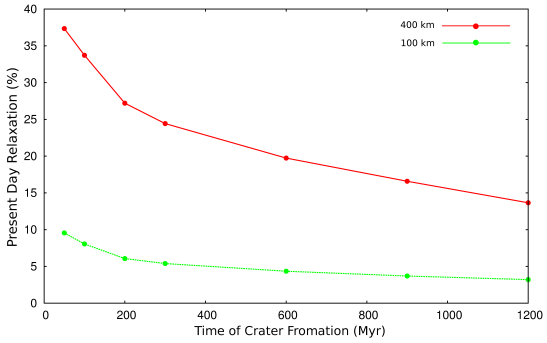

Figure 4: Modeled relaxation of a 400 km (red) and 100 km (green) diameter crater versus time of crater formation.

Discussion: Comparison of the observed with the predicted relaxation fractions shows that the thermal model underpredicts the amount of relaxation observed. Our observations show 100 km craters range from 0 - 40% relaxed while our model suggests a crater of this size could only be a maximum of 10% relaxed. We observe that craters larger than 250 km are all approximately 40% relaxed but this is only consistent with our model if all these craters formed almost directly after Rhea accreted. Clearly, there are systematic differences between our measured relaxation percentages and those predicted by the viscoelastic relaxation model.

One possible explanation for this discrepancy is that our model for Rhea is too cold. By assuming a relatively slow accretion timescale (2.9 Myr after CAI formation) we have reduced the role of 26Al in generating initially higher temperatures. A more rapid accretion timescale would result in higher temperatures and more relaxation. A second possible explanation is that Rhea may in fact be differentiated [15], although most interpretations of the gravity data show Rhea has a homogeneous interior [16]. If the silicates are concentrated at the center of Rhea, the temperatures in the ice shell above would be higher than in a uniform, undifferentiated body.

It is also possible that our estimates for initial crater depth are too deep and / or that modification processes other than viscous relaxation are in part responsible for reducing crater depth. This is likely the case for at least one of the craters we measured, which is unusually shallow possibly due to ejecta infill from nearby Tirawa (Figure 2).

Conclusions and future work: Our initial survey of 18 craters on Rhea has shown that while large craters appear relaxed, craters in the diameter range of 100 to 150 km appear to have a range of relaxation states. In general, the theoretical relaxation models underpredicted the observed relaxation, meaning that adjustments to the initial conditions for our models will be necessary, which may include faster accretion times or a differentiated Rhea.

Once we have completed our survey of Rhea, we will expand our work to other mid to large-sized icy satellites of Saturn as well as the Galilean satellites of Jupiter. Using the relaxation state of craters we will attempt to understand and compare the thermal histories of these moons. The USGS is currently testing camera models for Cassini ISS and Galileo SSI in SOCET SET, and we anticipate being able to construct alternate DEMs using SOCET SET in 2011.

References: [1] Dombard, A. J., and McKinnon W. B. (2006) JGR, 111 E01001; [2] Gaddis, L. et al. (1997) LPSC, 28, #387; [3] Moratto, Z. M. et al. (2010) LPSC XVI, #2364; [4] Schenk, P. M. (1989) JGR, 94, B4, 3813-3832; [5] Hale, W. S. and R. A. F. Grieve (1982) JGR, 87, A65-A76; [6] Thomas, P.J. and S.W. Squyres (1988) JGR, 93, 14919-14932 [7] Pike R. J. (1977) Impact and Explosion Cratering, Pergamon, New York; [8] Gault D.E. et al. (1975) JGR, 80, 2444-2464; [9] Zahnle K. et. al. (2003) Icarus 163, 263-289; [10] Matson D. et al. (2009) in Saturn from Cassini-Huygens, Springer NY; [11] Schubert, G. et al. (1981) Icarus 47, 46–59; [12] Amelin, Y. et al. (2002) Science 297, 1678–1683; [13] Castillo-Rogez, J. et al. 2007. Icarus 190, 179–202; [14] Zhong S.J. et al. (2003) G.J. Int. 155, 679-695; [15] Barr A.C. et al. (2008), LPSC 39, #2201; [16] Anderson, J. D. and G. Schubert (2007) GRL 34 L02202